

Fertilized egg cells secrete endopeptidases to avoid polytubey

<https://doi.org/10.1038/s41586-021-03387-5>

Received: 25 January 2020

Accepted: 24 February 2021

Published online: 31 March 2021

 Check for updates

Xiaobo Yu^{1,3}, Xuecheng Zhang^{1,3}, Peng Zhao^{1,3}, Xiongbo Peng¹, Hong Chen¹, Andrea Bleckmann², Anastasiia Bazhenova², Ce Shi¹, Thomas Dresselhaus^{2✉} & Meng-xiang Sun^{1✉}

Upon gamete fusion, animal egg cells secrete proteases from cortical granules to establish a fertilization envelope as a block to polyspermy^{1–4}. Fertilization in flowering plants is more complex and involves the delivery of two non-motile sperm cells by pollen tubes^{5,6}. Simultaneous penetration of ovules by multiple pollen tubes (polytubey) is usually avoided, thus indirectly preventing polyspermy^{7,8}. How plant egg cells regulate the rejection of extra tubes after successful fertilization is not known. Here we report that the aspartic endopeptidases ECS1 and ECS2 are secreted to the extracellular space from a cortical network located at the apical domain of the *Arabidopsis* egg cell. This reaction is triggered only after successful fertilization. *ECS1* and *ECS2* are exclusively expressed in the egg cell and transcripts are degraded immediately after gamete fusion. *ECS1* and *ECS2* specifically cleave the pollen tube attractor LURE1. As a consequence, polytubey is frequent in *ecs1 ecs2* double mutants. Ectopic secretion of these endopeptidases from synergid cells led to a decrease in the levels of LURE1 and reduced the rate of pollen tube attraction. Together, these findings demonstrate that plant egg cells sense successful fertilization and elucidate a mechanism as to how a relatively fast post-fertilization block to polytubey is established by fertilization-induced degradation of attraction factors.

Sexually reproducing organisms have established molecular mechanisms to prevent fertilization of an egg by more than one sperm (polyspermy). Polyspermy usually leads to lethal genome imbalance, genome dosage and chromosome segregation defects during further embryo development¹. Slow and fast blocks to polyspermy have been reported in animals that are associated with the cortical reaction⁴. Cortical granules are located in the cortex of the unfertilized mature egg, undergo exocytosis in a calcium-dependent manner to release their contents and are not renewed after successful fertilization⁴. Thus, to ensure monospermic fertilization of the egg, cortical granules are released upon sperm–egg interaction to generate a modified zona pellucida that surrounds and protects the egg or oocyte in most animal species studied. It has further been reported that protease activity is required to establish this block³.

Fertilization in flowering plants is more complex and involves an egg and a central cell. These cells are deeply embedded and protected by maternal tissues, and are neither accessible to swimming sperm nor contain a structure similar to the zona pellucida. As a new evolutionary acquisition, sperm cells lost their mobility and are transported as passive cargo by the pollen tube^{9,10}. This process involves cell–cell communication with the maternal tissues^{5,11}, culminating in bursting of the pollen tube inside the ovule, the release of two sperm cells and their fusion with an egg and a central cell, respectively, a process that is also known as double fertilization⁶. Similar to animals, polyspermy is very rare in plants^{12,13}. Monospermy occurs because usually only a single

pollen tube is guided inside the ovule to release its sperm cell cargo. It has previously been shown that synergid cells adjacent to the egg cell secrete chemoattractants such as EAI in maize¹⁴, LUREs in *Arabidopsis*¹⁵, and *Torenia*¹⁶ and XIUQIUS in *Arabidopsis*¹⁷ to guide the pollen tube towards the egg cell. Once the first pollen tube delivers a pair of sperm cells¹⁸ and double fertilization is achieved, entry of other pollen tubes into the micropyle of the ovule (polytubey) is prevented. In *Arabidopsis*, this block to polytubey is initiated by the accumulation of nitric oxide during the arrival of a pollen tube to the micropyle, leading to modification of LURE1 and thus blocking its secretion and interaction with its receptor¹⁹. Notably, single fertilization does not prevent polytubey, indicating that both egg and central cells contribute to this block⁸. It was later shown that the fertilized central cell fuses with the persistent synergid cells and thus removes the source of the attractant²⁰, which can be considered as a slow block to polytubey. If fertilization fails, a recovery mechanism that is activated with some delay and by which the persistent synergid cell continues to attract pollen tubes to ensure successful double fertilization has previously been reported^{7,21}. How plant egg cells (1) sense successful fertilization and (2) contribute to the rejection of secondary pollen tubes, and (3) whether there exists a fast block to polytubey and (4) whether a cortical reaction takes place in the egg cell that is mechanistically comparable to animals, are not known. Granules containing the sperm cell activator EC1 have been reported to be released from egg cells, but this occurs before gamete fusion²² and is thus not comparable with the cortical reaction in animals.

¹State Key Laboratory of Hybrid Rice, College of Life Sciences, Wuhan University, Wuhan, China. ²Cell Biology and Plant Biochemistry, University of Regensburg, Regensburg, Germany. ³These authors contributed equally: Xiaobo Yu, Xuecheng Zhang, Peng Zhao. ✉e-mail: thomas.dresselhaus@ur.de; mxsun@whu.edu.cn

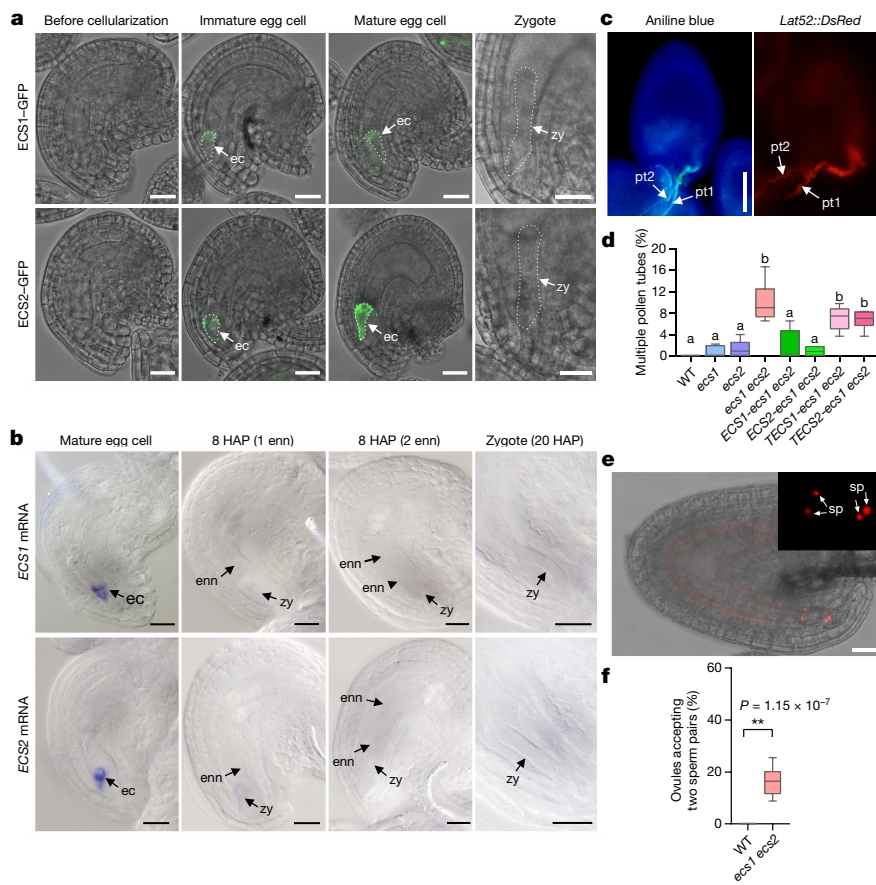


Fig. 1 | Egg cell-specific ECS1 and ECS2 act together to prevent polytubey in *Arabidopsis*. **a**, ECS1–GFP and ECS2–GFP were detected in the egg cell (ec) after cellularization of the embryo sac. Signals disappeared during zygote (zy) elongation. **b**, *ECS1* and *ECS2* mRNAs were specifically located in egg cells and degraded immediately after fertilization (arrows). enn, endosperm nucleus. **c**, Polytubey in *ecs1 ecs2* double-mutant ovules shown by aniline blue staining (left) and by using *LAT52::DsRed* labelling (right). Arrows indicate pollen tubes (pt). **d**, Proportions of polytubey in *ecs1* and *ecs2* single mutants as well as *ecs1 ecs2* double mutants at 24 HAP. TECS1 and TECS2 indicate the truncated *ECS1* and *ECS2* versions that lack the signal peptide ($n = 484$ for wild type (WT); 301 for *ecs1*; 312 for *ecs2*; 501 for *ecs1 ecs2*; 303 for *TECS1-ecs1 ecs2*; 306 for *ECS2-ecs1 ecs2*; 308 for *TECS1-ecs1 ecs2*; and 315 for *TECS2-ecs1 ecs2*). The same

letters above the bars indicate lack of significant differences according to Tukey–Kramer multiple comparison test (one-way analysis of variance (ANOVA) between groups; $P = 4.2 \times 10^{-15}$; $F = 27.13$). $P < 0.05$ was considered significant. **e**, Additional sperm cell (sp) pairs were observed in *ecs1 ecs2* at 24 HAP. **f**, The proportions of additional sperm pairs in ovules of *ecs1 ecs2* mutants after fertilization ($n = 315$ for WT; 886 for *ecs1 ecs2*). **Statistical difference compared to WT (two-tailed Student’s *t*-test; $P < 0.01$). Data in **d**, **f** are presented in box-and-whisker plots: centre line represents the 50th percentile; bottom and top of each box indicate the 25th and 75th percentiles, respectively; and whiskers represent minimum and maximum. Scale bars, 20 μm (**a**, **b**, **e**) and 100 μm (**c**).

To address these questions, we studied two genes of the model plant *Arabidopsis thaliana* that are specifically expressed in egg cells and the products of which were predicted to be secreted. On the basis of their expression pattern (Fig. 1, Extended Data Fig. 1a), they were named *EGG CELL-SPECIFIC1* (*ECS1*) and *ECS2*. Promoter activity and analysis of ECS–GFP fusion protein reporter lines confirmed that *ECS1* and *ECS2* are specifically expressed in egg cells (Fig. 1a, Extended Data Fig. 1b–i). *ECS1*–GFP and *ECS2*–GFP fusion protein signals were detected in immature egg cells immediately after cellularization of the embryo sac. The GFP signal decreased rapidly after fertilization and disappeared after zygote division (Fig. 1a). In situ hybridization showed that *ECS1* and *ECS2* mRNAs are specifically located in egg cells and degraded quickly after fertilization (Fig. 1b), implying that mRNA degradation was triggered by fertilization. *ECS1* and *ECS2* encode members of the highly specific family of A1 aspartic endopeptidases that contain a signal peptide for entering the secretory pathway and two typical activity sites: DTGS and DSGT (Extended Data Fig. 2a). Their closest homologue is the A1 family endopeptidase CDR1 (Extended Data Fig. 2b), which is involved in the regulation of disease resistance²³.

To explore the roles of *ECS1* and *ECS2*, we analysed T-DNA insertion alleles designated as *ecs1-1*, *ecs1-2*, *ecs2-1* and *ecs2-2* (Extended Data Fig. 2c, d). Both *ecs1* and *ecs2* homozygous mutants grew normally, lacking any obvious reproductive defect. Owing to their identical expression pattern, we created two independent double mutants, *ecs1-1 ecs2-1* and *ecs1-2 ecs2-2*, both of which displayed similar polytubey phenotypes. Secondary pollen tubes entered the embryo sac in approximately 10% of ovules (Fig. 1c, d). Both *ECS1* and *ECS2* were able to restore the polytubey phenotype of *ecs1 ecs2* double mutants, indicating a redundant role in preventing the entry of multiple pollen tubes (Fig. 1d). Gamete fusion failure has previously been reported to result in polytubey^{7,21}. We therefore investigated whether defects in gamete fusion also occur in *ecs1 ecs2* mutants. By using a *HTR10::HTR10-mRFP* marker line that labels sperm cell nuclei, we observed normal rates of fertilization of both female gametes in *ecs1 ecs2*-mutant ovules. However, about 16.4% of ovules showed an occurrence of extra pairs of sperm cells as early as 6–8 h after pollination (HAP) (Fig. 1e, f, Extended Data Fig. 3). These findings reveal that *ECS1* and *ECS2* are involved in preventing polytubey only after successful fertilization.

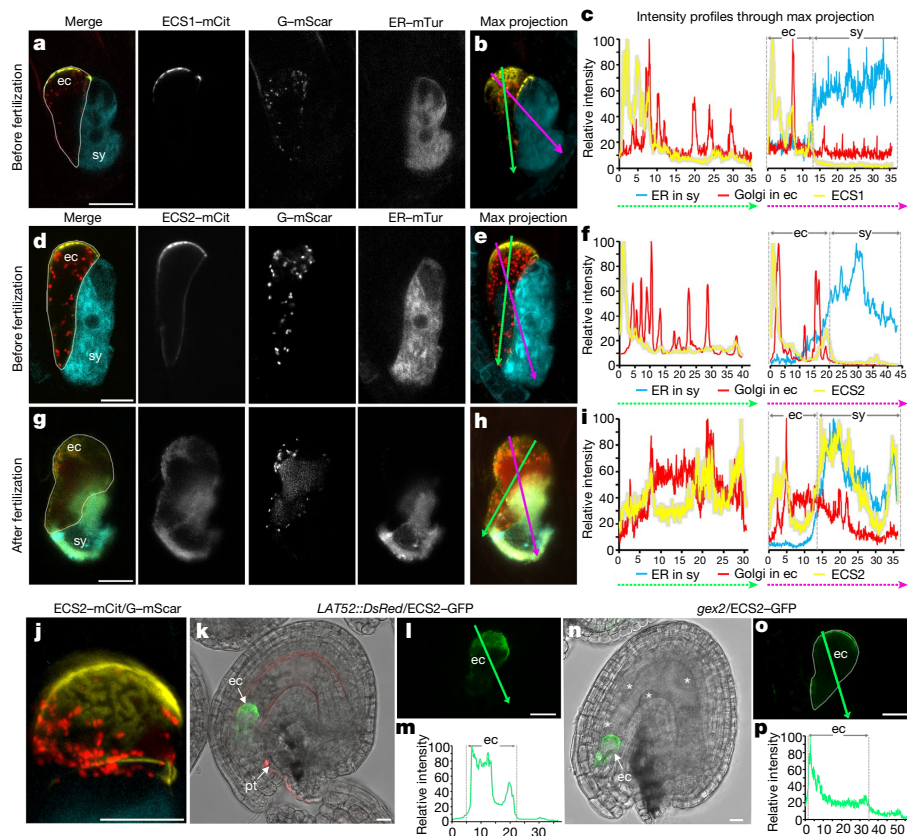


Fig. 2 | ECS proteins are secreted from the egg cell after successful sperm-egg cell fusion. a–f, ECS1–mCitrine (a–c) and ECS2–mCitrine (d–f) accumulated at the apical domain of mature egg cells forming a net-like structure before fertilization. **g–i**, ECS2–mCitrine was secreted from the fertilized egg cell to the extracellular space. **In a, d, g**, merged images of ECS1/2–mCitrine (ECS–mCit), the egg cell expressed Golgi–mScarlet (G–mScar) and the synergid cell (sy) expressed endoplasmic reticulum-tagged mTurquoise2 (ER–mTur) as indicated. **In b, e, h**, maximal projection of imaged cells is shown. **In c, f, i**, intensity plot profiles along the egg cell (green arrow) and the egg cell apparatus (magenta arrow) are shown. **j**, Z-stack showing an

enlargement of the apical ECS2–mCit network before fertilization. **k–m**, Entrance of a DsRed-labelled pollen tube into the ovule did not trigger ECS2–GFP secretion. The plot profile shows the relative fluorescence signal intensities (green line) along a dashed line drawn across the egg and synergid cells (indicated in **l**). **n–p**, Single fertilization of the central cell using pollen from *gex2* mutants did not trigger ECS2–GFP secretion. Single fertilization was indicated by the occurrence of four endosperm nuclei (asterisks). For the plots in **c, f, i, m, p**, x axis indicates distances along the dashed line measured in μm and y axis indicates the relative fluorescent signal intensities of mCit (yellow line), mTur (cyan line), mScarlet (red line) and GFP (green line). Scale bars, 10 μm.

To investigate the molecular mechanism of how the function of ECS is capable of preventing polytubey, we analysed the dynamic distribution of their GFP and mCitrine fusion proteins, respectively, during the entire fertilization process. Both ECS1 and ECS2 were secreted from the egg cell only after successful fertilization (Fig. 2, Extended Data Fig. 4). By using a triple marker that labelled ECS1 and ECS2, the cytoplasm of the egg cell and the cytoplasm of the synergid cells, respectively, we found that vesicles containing ECS1 and ECS2 accumulated in mature egg cells in an apical network at the plasma membrane (Fig. 2a–f, j, Extended Data Fig. 4a–d, i–l). During fertilization, ECS1 and ECS2 were almost completely secreted towards the degenerating synergid cell (Fig. 2g–i, Extended Data Fig. 4e–h). The cortical network disappeared, was not renewed and the remaining ECS signals inside the fertilized egg cell appeared weak. To investigate the timing of ECS release, we next used pollen tubes expressing *LAT52::DsRed* or *HTR10::HTR10-mRFP* to monitor the distribution of ECS during fertilization. We found that entry of pollen tubes into ovules (Fig. 2k–m, Extended Data Fig. 4m, n), synergid cell degeneration and sperm cell release were not sufficient to trigger ECS secretion from the egg cell. ECS secretion was triggered only by sperm–egg fusion. To confirm this observation, we used *gcs1*-mutant pollen, the sperm cells of which could not fuse with egg and central cells²⁴, to pollinate ECS2–GFP pistils. Although sperm cells were successfully released, gamete fusion failed and ECS

was not secreted from the egg cell (Extended Data Fig. 4o, p). We next examined ECS secretion after single fertilization of the central cell. We used *gex2*-mutant pollen that is defective in sperm–egg adhesion²⁵ to pollinate ECS2–GFP pistils. We found that sperm–central cell fusion, as indicated by the presence of multiple endosperm nuclei, did not trigger ECS secretion from the egg cell (Fig. 2n–p), further indicating that ECS secretion is dependent on successful sperm–egg cell fusion. Finally, we tested whether truncated versions of ECS1 and ECS2 that lacked the signal peptide were secreted from egg cells. As shown in Fig. 1d and Extended Data Fig. 5, the truncated versions of ECS1 and ECS2 did not recover the *ecs1 ecs2* double mutant polytubey phenotype and were retained in the egg cell during fertilization.

To understand the role of ECS secretion in blocking polytubey after fertilization, we tested whether the two endopeptidases are capable of binding and cleaving pollen tube attractants. Pull-down assays confirmed specific interaction between LURE1.2 and ECS1, and LURE1.2 and ECS2 (Fig. 3a). This suggested that LURE1 pollen tube attractors are direct substrates of ECS1 and ECS2. To investigate whether they are capable of cleaving the LURE1 attractant, ECS1 or ECS2 and LURE1.2 were transiently co-expressed in *Nicotiana benthamiana* leaves and human embryonic kidney (HEK293T) cells, respectively. We observed that the protein levels of LURE1 were significantly lower when co-expressed with ECS in both mammal cells and *N. benthamiana* leaves (Fig. 3b,

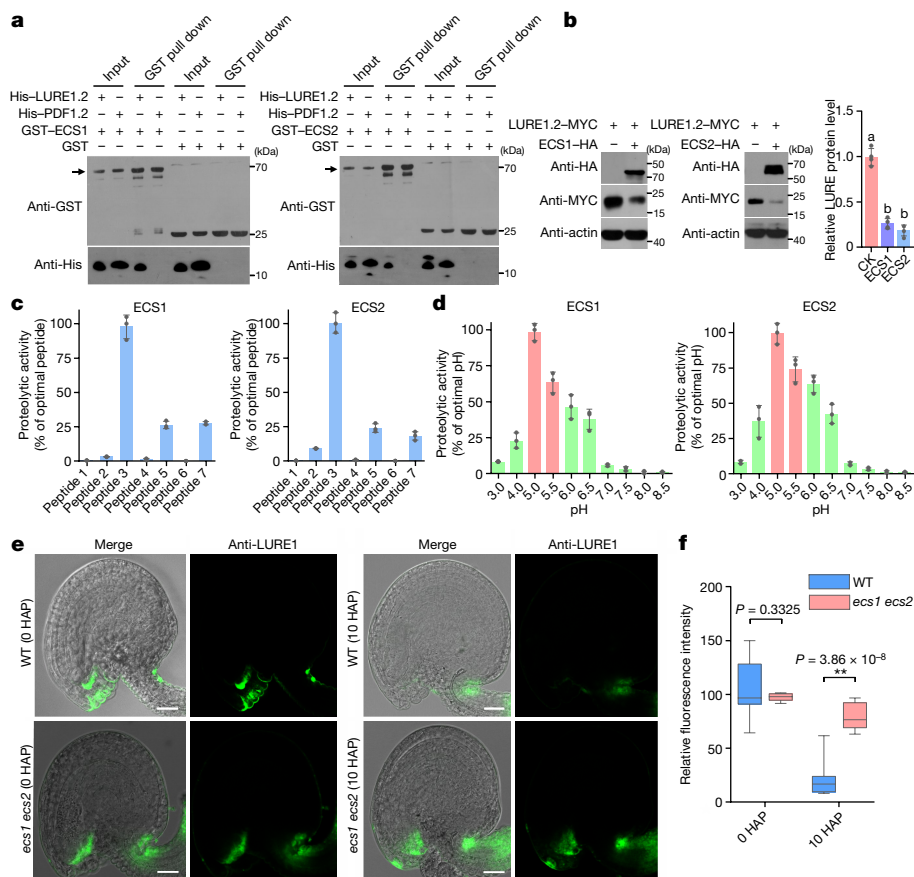


Fig. 3 | The LURE1.2 pollen tube attractant is a direct target and substrate of ECS1 and ECS2 endopeptidases. **a**, ECS1 and ECS2 interacted with LURE1.2, but not with PDF1.2, in pull-down assays. Arrows indicate glutathione S-transferase (GST)–ECS1/2 fusion proteins. His, histidine. **b**, LURE1.2 was degraded by co-expressed ECS1 and ECS2 in leaves of *N. benthamiana*. Histograms show relative protein levels of LURE1.2. Protein levels of LURE1.2 co-expressed with an empty vector were used as control (CK). Mean \pm s.d. from four independent experiments. The same letters indicate lack of significant differences according to Tukey–Kramer multiple comparison test (one-way ANOVA between groups; $P = 1.22 \times 10^{-7}$; $F = 150.24$). HA, haemagglutinin. **c**, Proteolytic activity of recombinant ECS1 and ECS2 on different fluorogenic peptide fragments (peptides 1–7). See Supplementary Fig. 8 for details. Relative cleavage activity of ECS1 against each LURE peptide is shown as relative percentage of peptide 3, which was set to 100%. **d**, The effects of pH on

proteolytic activities of ECS1 and ECS2 against LURE1 peptide 3 as substrate. Data in **c**, **d** are mean \pm s.d. of three independent experiments. **e**, Immunofluorescence study showing that LURE1 amounts and localization were unchanged after fertilization in the *ecs1 ecs2* double mutant. Before fertilization (0 HAP), LURE1 accumulated at the micropylar region and the surface of the funiculus in both WT and *ecs1 ecs2* mutant ovules. Shortly after fertilization (10 HAP), LURE1 was much weaker in WT ovules but still present at comparable levels in mutant ovules. Scale bars, 20 μ m. **f**, Quantification of green fluorescence intensity in ovules from WT and *ecs1 ecs2* mutants at stages shown in **e** ($n = 10$). In box-and-whisker plots, centre line represents the 50th percentile; bottom and top of each box indicate 25th and 75th percentiles, respectively; and whiskers represent the minimum and maximum. **Statistical difference compared to WT (two-tailed Student’s *t*-test; $P < 0.01$).

Extended Data Fig. 6a, b), indicating that ECS1 and ECS2 are capable of cleaving, and thus inactivating, LURE1s. Proteolytic fragments were not detected, further indicating that extracellular LURE1s are stable, but are quickly degraded by non-specific proteases after specific cleavage by ECS endopeptidases. To identify the cleavage site, we synthesized seven fluorogenic peptide substrates according to the LURE1.2 protein sequence (Extended Data Fig. 6c, d). Proteolytic activity of recombinant ECS against these fluorogenic peptide substrates was directly measured (Fig. 3c, Extended Data Fig. 6e). ECS efficiently cleaved LURE1.2 peptide substrates 3, 5 and 7, which are located at the middle and C-terminal regions of LURE1.2 (Extended Data Fig. 6d, g). ECS1 and ECS2 share similar biochemical characteristics: peptide substrate 3 was preferentially cleaved at a pH optimum of 5. Both enzymes were inactive at pH 7 and above (Fig. 3d, Extended Data Fig. 6f). Notably, peptide 3, which showed the highest cleavage rate, is a conserved region within LURE1.1–LURE1.5, but is lacking in LURE1.7 and LURE1.8 and recently reported XIUQIUs, resembling weaker and less specific pollen tube attractors in *Arabidopsis*¹⁷.

To confirm that ECS1 and ECS2 could cleave LURE1 in vivo, protein levels of endogenous LURE1 and LURE1–GFP in wild-type and *ecs1 ecs2* mutant ovules were compared before and after fertilization using immunofluorescence and LURE1–GFP analyses. LURE1 protein levels were comparable during pollination, but quickly decreased shortly after fertilization (at 10 HAP, which is about 2–4 h after fertilization) in wild-type ovules and remained almost unchanged in *ecs1 ecs2* ovules (Fig. 3e, f, Extended Data Fig. 7a, b). An in vitro pollen tube attraction assay using gelatin beads showed that attraction was lost when beads contained both LURE1.2 and ECS endopeptidases (Extended Data Fig. 7c). Together, these findings confirm that ECS activity is required to remove the pollen tube attractant LURE1 shortly after successful fertilization.

To finally show that ECS-mediated LURE1 degradation is critical for blocking pollen tube entrance to susceptible ovules and to demonstrate applications for manipulating attraction, ECS1 and ECS2 were ectopically expressed in synergid cells driven by the synergid cell-specific *DD31* promoter²⁶. In contrast to the triggered secretion of ECS–GFP in egg cells, endopeptidases appeared to be constitutively secreted to the

filiform apparatus in synergid cells (Extended Data Fig. 8a). Immunofluorescence and LURE1.2–GFP analyses revealed that the protein levels of LURE1.2 were significantly decreased (Extended Data Fig. 8b, c, f–i). Moreover, while more than 50% of wild-type ovules were already targeted by pollen tubes at 6 HAP, less than 10% of pollen tube attraction were observed in both *DD31::ECS1* and *DD31::ECS2* ectopic expression lines (Extended Data Fig. 8d, e, j–l). These numbers are comparable to that of mutants lacking all *LURE1* genes²⁵ at 4–6 HAP, and thus indicate that ECS-mediated LURE1 degradation is critical for pollen tube attraction. Ectopic expression of the truncated versions of *ECS1* and *ECS2* or of the egg cell-expressed subtilisin-like protease *SBT4.13* (ref.²⁷) in synergid cells had no significant effects on the protein levels of LURE1.2 and on the rate of pollen tube attraction (Extended Data Fig. 9). Finally, we confirmed that the endopeptidase activity of ECS1 and ECS2 was required to prevent polytubey. The active sites of the proteins were mutated, protease activity was measured using peptide 3 of LURE1 and the *ecs1 ecs2* mutant was complemented with mutated versions. In contrast to wild-type ECS endopeptidases, the mutant versions lacked proteolytic activity and were not capable of rescuing the mutant phenotype (Extended Data Fig. 10).

In summary, we demonstrated that two aspartic endopeptidases, ECS1 and ECS2, were exclusively expressed in egg cells, accumulated in a cortical network and were rapidly secreted as a response to successful sperm–egg cell fusion. This reaction has similarities to the cortical reaction in animals, which is triggered by calcium²⁸. Elevations in calcium levels correlated with sperm–egg fusion were reported in plants more than 20 years ago during *in vitro* fertilization studies in maize^{29,30} and were recently confirmed *in vivo* in *Arabidopsis*, showing a short elevation for a few minutes immediately after successful membrane fusion^{31,32}. Whether these trigger the release of ECS is likely but has to be determined in further experimentation. Thus, despite strong morphological differences and lack of mobile sperm and a zona pellucida, the concept of fertilization-induced release of proteases to prevent polyspermy appears to be conserved between animals and plants. ECS proteases contribute to the block of polytubey, but the amount of the pollen tube attractants LURE1 and XIUQIUs can also be reduced when the persistent synergid cell fuses with the large endosperm cell, which ultimately terminates pollen tube attraction²⁰. However, this is a slower block and does not remove extracellular attraction factors. Thus, single fertilization of either the egg cell or the central cell is not sufficient to establish a complete block to polytubey as both cells contribute to the block⁸. Moreover, blocks to polytubey are only about 96% effective in maize¹² and 98% in *Arabidopsis*^{7,8}, indicating that weaker attractants that might not be effectively degraded by ECS endopeptidases or inactivated by nitric oxide¹⁹ can still lead to pollen tube attraction at a low frequency. Considering that polyspermy in plants occurs at a very low rate^{12,13}, and thus significantly less frequent than polytubey, there probably also exists a fast mechanism to prevent polyspermy after delivery of sperm cells. Cell wall material is released after gamete fusion *in vitro*³³ and probably represents an ultimate block.

Whether ECS1 and ECS2 are also capable of degrading additional proteins involved in the regulation of gamete activation, adhesion, fusion and the establishment of a cell wall block remain to be shown in further experimentation. Other egg cell-expressed proteases such as the above-mentioned *SBT4.13* might contribute, although their target proteins are yet to be identified. In conclusion, we have elucidated a concept of a relatively fast block to show how plants avoid fusion of egg cells by multiple sperm via fertilization-induced release of endopeptidases that specifically degrade pollen tube attractors and thereby prevent polytubey.

Online content

Any methods, additional references, Nature Research reporting summaries, source data, extended data, supplementary information,

acknowledgements, peer review information; details of author contributions and competing interests; and statements of data and code availability are available at <https://doi.org/10.1038/s41586-021-03387-5>.

- Wong, J. L. & Wessel, G. M. Defending the zygote: search for the ancestral animal block to polyspermy. *Curr. Top. Dev. Biol.* **72**, 1–151 (2006).
- Burkart, A. D., Xiong, B., Baibakov, B., Jiménez-Movilla, M. & Dean, J. Ovastacin, a cortical granule protease, cleaves ZP2 in the zona pellucida to prevent polyspermy. *J. Cell Biol.* **197**, 37–44 (2012).
- Vacquier, V. D., Tegner, M. J. & Epel, D. Protease activity establishes the block against polyspermy in sea urchin eggs. *Nature* **240**, 352–353 (1972).
- Liu, M. The biology and dynamics of mammalian cortical granules. *Reprod. Biol. Endocrinol.* **9**, 149 (2011).
- Johnson, M. A., Harper, J. F. & Palanivelu, R. A fruitful journey: pollen tube navigation from germination to fertilization. *Annu. Rev. Plant Biol.* **70**, 809–837 (2019).
- Dresselhaus, T., Sprunck, S. & Wessel, G. M. Fertilization mechanisms in flowering plants. *Curr. Biol.* **26**, R125–R139 (2016).
- Beale, K. M., Leydon, A. R. & Johnson, M. A. Gamete fusion is required to block multiple pollen tubes from entering an *Arabidopsis* ovule. *Curr. Biol.* **22**, 1090–1094 (2012).
- Maruyama, D. et al. Independent control by each female gamete prevents the attraction of multiple pollen tubes. *Dev. Cell* **25**, 317–323 (2013).
- Zhang, J. et al. Sperm cells are passive cargo of the pollen tube in plant fertilization. *Nat. Plants* **3**, 17079 (2017).
- Glöckle, B. et al. Pollen differentiation as well as pollen tube guidance and discharge are independent of the presence of gametes. *Development* **145**, dev152645 (2018).
- Zhou, L. Z. & Dresselhaus, T. Friend or foe: signaling mechanisms during double fertilization in flowering seed plants. *Curr. Top. Dev. Biol.* **131**, 453–496 (2019).
- Grossniklaus, U. Polyspermy produces tri-parental seeds in maize. *Curr. Biol.* **27**, R1300–R1302 (2017).
- Nakel, T. et al. Triparental plants provide direct evidence for polyspermy induced polyploidy. *Nat. Commun.* **8**, 1033 (2017).
- Márton, M. L., Cordts, S., Broadhvest, J. & Dresselhaus, T. Micropylar pollen tube guidance by egg apparatus 1 of maize. *Science* **307**, 573–576 (2005).
- Takeuchi, H. & Higashiyama, T. A species-specific cluster of defensin-like genes encodes diffusible pollen tube attractants in *Arabidopsis*. *PLoS Biol.* **10**, e1001449 (2012).
- Okuda, S. et al. Defensin-like polypeptide LUREs are pollen tube attractants secreted from synergid cells. *Nature* **458**, 357–361 (2009).
- Zhong, S. et al. Cysteine-rich peptides promote interspecific genetic isolation in *Arabidopsis*. *Science* **364**, eaau9564 (2019).
- Sandaklie-Nikolova, L., Palanivelu, R., King, E. J., Copenhaver, G. P. & Drews, G. N. Synergid cell death in *Arabidopsis* is triggered following direct interaction with the pollen tube. *Plant Physiol.* **144**, 1753–1762 (2007).
- Duan, Q. et al. FERONIA controls pectin- and nitric oxide-mediated male-female interaction. *Nature* **579**, 561–566 (2020).
- Maruyama, D. et al. Rapid elimination of the persistent synergid through a cell fusion mechanism. *Cell* **161**, 907–918 (2015).
- Kasahara, R. D. et al. Fertilization recovery after defective sperm cell release in *Arabidopsis*. *Curr. Biol.* **22**, 1084–1089 (2012).
- Sprunck, S. et al. Egg cell-secreted EC1 triggers sperm cell activation during double fertilization. *Science* **338**, 1093–1097 (2012).
- Simões, I., Faro, R., Bur, D. & Faro, C. Characterization of recombinant CDR1, an *Arabidopsis* aspartic proteinase involved in disease resistance. *J. Biol. Chem.* **282**, 31358–31365 (2007).
- Mori, T., Kuroiwa, H., Higashiyama, T. & Kuroiwa, T. GENERATIVE CELL SPECIFIC 1 is essential for angiosperm fertilization. *Nat. Cell Biol.* **8**, 64–71 (2006).
- Mori, T., Igawa, T., Tamiya, G., Miyagishima, S. Y. & Berger, F. Gamete attachment requires GEX2 for successful fertilization in *Arabidopsis*. *Curr. Biol.* **24**, 170–175 (2014).
- Steffen, J. G., Kang, I. H., Macfarlane, J. & Drews, G. N. Identification of genes expressed in the *Arabidopsis* female gametophyte. *Plant J.* **51**, 281–292 (2007).
- Bleckmann, A. & Dresselhaus, T. Whole mount RNA-FISH on ovules and developing seeds. *Methods Mol. Biol.* **1669**, 159–171 (2017).
- Zimmerberg, J. & Whitaker, M. Irreversible swelling of secretory granules during exocytosis caused by calcium. *Nature* **315**, 581–584 (1985).
- Antoine, A. F. et al. A calcium influx is triggered and propagates in the zygote as a wavefront during *in vitro* fertilization of flowering plants. *Proc. Natl Acad. Sci. USA* **97**, 10643–10648 (2000).
- Digonnet, C., Aldon, D., Leduc, N., Dumas, C. & Rougier, M. First evidence of a calcium transient in flowering plants at fertilization. *Development* **124**, 2867–2874 (1997).
- Denninger, P. et al. Male–female communication triggers calcium signatures during fertilization in *Arabidopsis*. *Nat. Commun.* **5**, 4645 (2014).
- Hamamura, Y. et al. Live imaging of calcium spikes during double fertilization in *Arabidopsis*. *Nat. Commun.* **5**, 4722 (2014).
- Kranz, E., von Wiegand, P. & Lörz, H. Early cytological events after induction of cell division in egg cells and zygote development following *in vitro* fertilization with angiosperm gametes. *Plant J.* **8**, 9–23 (1995).

Publisher's note Springer Nature remains neutral with regard to jurisdictional claims in published maps and institutional affiliations.

© The Author(s), under exclusive licence to Springer Nature Limited 2021

Methods

Plant materials and growth conditions

T-DNA insertion lines SALK_021086 (*ecs1-1*), SALK_006574 (*ecs1-2*), SALK_090795 (*ecs2-1*), SALK_036333 (*ecs2-2*) and *gcs1* (SALK_135496) were obtained from the *Arabidopsis* Biological Resource Center (ABRC). *gex2* (FLAG_441D08) was obtained from the Versailles *Arabidopsis* Stock Center. The *LATS2::DsRed* maker line was provided by Y. Zhang (University of Shandong Agricultural University). The *LATS2::GUS* maker line was provided by C. Li (East China Normal University). *Arabidopsis thaliana* Columbia-0 (Col-0) was used as the WT control. Plants were grown in soil in a greenhouse or in indoor growth rooms under long-day conditions (16 h light/8 h dark) at 22 °C.

Protein sequence analysis

Sequence alignment of ECS1 (At1G31450), ECS2 (AT2G35615) and CDRI (AT5G33340) protein sequences was performed using the CLUSTAL X2 software. Prediction of the ECS signal peptide was performed using SUBA3 (<http://suba.plantenergy.uwa.edu.au/>), TargetP (<http://www.cbs.dtu.dk/services/TargetP/>) and iPSORT (<http://ipsort.hgc.jp/>) software.

Vector construction and plant transformation

To generate the pECS::ECS–GFP fusion construct, a DNA fragment containing the promoter and coding sequence was amplified from *A. thaliana* ecotype Col-0 genomic DNA and inserted into the P094 vector. To generate the pECS::H2B–GFP construct, the promoter region was amplified and inserted into the P095 vector. To generate the pECS::ECS complementation construct, *ECS* genomic DNA containing the promoter, coding sequence and 3' untranslated region was amplified and inserted into the P092 vector. *DD31::ECS1-GFP* and *DD31::ECS2-mRFP* were generated on the basis of the P094 vector³⁴. The triple marker lines expressing pECS1/2::ECS1/2–mCitrine, *LRE::ER-mTurquoise2* and *EC1.1::Golgi-mScarlet* were generated by Golden Gate assembly using the Green Gate Cloning System³⁵ and pGGZ003 as the destination plasmid. A list of used modules, their source and tagging site are provided in Supplementary Table 2. The compartment marker is based on markers for colocalization studies³⁶. The coding sequence of the endoplasmic reticulum and Golgi marker proteins were expressed under cell-type-specific promoters.

All primers used for vector construction are listed in Supplementary Table 1. All constructs were transferred into *Agrobacterium tumefaciens* strain GV3101, and *Arabidopsis* transformation was performed according to a previously described protocol³⁷.

LURE1 antibody preparation and immunofluorescence

The coding region of *LURE1.2* lacking the signal peptide sequence was cloned and inserted into the pSmart-I vector. Recombinant *LURE1.2* produced in *Escherichia coli* was purified as antigen. *LURE1.2* antibodies were produced in rabbits by DIA-AN. For western blotting, total proteins were subjected to SDS–PAGE and transferred to nitrocellulose membranes for immunoblotting. For immunofluorescence analysis, ovules were collected and fixed in 4% paraformaldehyde for 12 h, washed three times with PBS and incubated in PBS containing 3% Nonidet P-40 for 1 h to enhance permeability. Ovules were then washed and incubated for 2 h at 25 °C with an anti-*LURE1* antibody (1:50 dilution). Afterwards, samples were washed three times (15 min each) in PBS and incubated for 2 h with a goat anti-rabbit Alexa Fluor 488-conjugated secondary antibody (Thermo Fisher Scientific).

In situ hybridization

RNA probes for in situ hybridization were generated as follows: a 556-bp fragment of the 3' UTR region of *ECS1* and a 317-bp 5' UTR region of *ECS2* were amplified from genomic DNA of *A. thaliana* Col-0 using primers listed in Supplementary Table 1. Purified PCR products were cloned into

the pGGC000 vector. Next, DNA was linearized using *AseI* restriction enzyme (New England Biolabs), purified using NucleoSpin Gel and a PCR Clean-up kit (both Macherey-Nagel) according to the manufacturer recommendations. DIG-labelled antisense and sense RNA probes were synthesized using the DIG RNA Labelling Kit (Merck) with T7 and SP6 polymerase, respectively. RNA was precipitated by LiCl and stored at –80 °C until usage. Ovule samples were prepared and fixed, and further in situ hybridization steps were carried out as described²⁷.

Confocal microscopy and image analysis

Ovules were observed using a confocal microscope (Leica TCS SP8) or Spinning Disc microscope (Visitron system VisiScope) using a HC PL APO ×63/1.4 NA oil DIC objective. The average fluorescent intensity of ovules was measured using the LAS-X software v.X3.5.5.19976 (Leica) or FIJI v.1.53c (<https://imagej.net/Fiji>). Volume projections of Z-stacks were created by IMARIS v.X649.31. For FM4-64 staining, dissected ovules were incubated for 10 min in a 50 μM staining solution in PBST puffer before imaging and measurements. For in situ hybridization, ovules were imaged using an Axiocam105 colour camera mounted to an Imager M2 microscope (Zeiss) by using a Plan-Apochromat ×40/1.4 NA oil DIC objective.

Pollination and pollen tube observation

WT pollen and other marker lines were pollinated to emasculated WT and *ecs1 ecs2*-mutant pistils. Pistils were collected at precise time points from 5 to 24 HAP for visualization of pollen tube behaviour, sperm cell release and determination of fertilization rates. For aniline blue staining, pistils were fixed in Carnoy's fixative (ethanol:acetic acid 3:1). Aniline blue staining was then performed according to a previously described protocol³⁸. *LATS2::DsRed* and *LATS2::GUS* maker lines were used to visualize pollen tube behaviour. Pistils pollinated with *LATS2::DsRed*-expressing pollen were collected and observed under a confocal microscope. Pistils pollinated with *LATS2::GUS*-expressing pollen were collected and observed after GUS staining³⁴.

In vivo examination of ESC activity and LURE degradation

For transient expression of *ESC1* and *LURE1.2* in *N. benthamiana* leaves, full-length coding sequences of *ESC1* and *LURE1* (without signal peptide sequences and stop codons) were amplified and inserted in-frame with 6×-HA and 6×-MYC into the pART27 vector downstream of the 35S promoter to generate the 35S::*ESC1-6x-HA* and 35S::*LURE1.2-6x-MYC* expression vectors, respectively. All constructs were transferred into *A. tumefaciens* strain GV3101 and transiently expressed in *N. benthamiana* leaves. Transient expression was assayed as previously described³⁹. *Nicotiana benthamiana* leaves were collected 48 h after infiltration and ground into powder for protein extraction. Total proteins were extracted in buffer containing 20 mM Tris-HCl (pH 7.5), 150 mM NaCl, 1 mM PMSF and protease inhibitor cocktail (1:50; Roche). Total proteins were then subjected to SDS–PAGE and subsequent western blotting. For transient expression of *ESCs* and *LURE1.2* in HEK293T cells, full-length coding sequences of *ESC* and *LURE1.2* (without signal peptide sequences and stop codons) were amplified and inserted into the pHAGE-puro vector. Constructs were then transfected into HEK293T cell lines using Lipofectamine 3000 reagent (Thermo Fisher Scientific). Cells were collected 36 h after transfection for protein extraction and subsequent immunoblotting. Antibodies including anti-HA (1:2,000 dilution; Abclonal), anti-MYC (1:2,000; Abclonal), anti-actin (1:2,000 dilution; Abbkine) and anti-GAPDH (1:2,000 dilution; Abclonal) were used for western blotting experiments.

Recombinant protein expression and purification

The *LURE1.2* coding sequence without signal peptides was amplified and cloned into pET-32a. The generated vector was transformed into *E. coli* strain BL21 (DE3). Recombinant *LURE1.2* was expressed and purified according to the PET system instructions. The coding region of *ESC*

without putative signal peptide sequences (Extended Data Fig. 2a) was amplified and inserted into the pPIC9K vector (Invitrogen). Plasmid DNA was linearized and electroporated into *Pichia pastoris* (GS115) cells according to the manufacturer's instructions. Yeast was grown in buffered glycerol complex (BMGY) medium and transferred into buffered methanol complex (BMMY) medium with 0.5% methanol for expression induction when optical density at 600 nm (OD_{600}) reached 2.5. After 3 days of induction, medium was collected for protein purification. Recombinant ECS proteins were purified using Ni-NTA His Bind Resin (Merck) according to the manufacturer's instructions.

In vitro pollen tube attraction assay

For the in vitro attraction assay, recombinant LURE (1 μ M) was mixed with recombinant ECS proteases (1 μ M) and then incubated at 37 °C for 0.5 h. Mixtures were diluted 200 times and used to prepare gelatin beads in an assay as previously described¹⁵.

ECS1 and ECS2 proteolytic activity assay

To investigate the proteolytic activity of recombinant ECS1 and ECS2 against LURE1.2, fluorogenic LURE1 peptide substrates were designed, synthesized (GenScript) and used for proteolytic activity determination. Peptides were labelled with MCA and DNP at both ends, which is a well-established procedure to study endopeptidase activities^{23,40}. To determine optimal LURE substrates for ECS1 and ECS2, ECS activity was measured using a series of fluorogenic LURE1 peptide substrates in a reaction mixture containing 50 mM sodium phosphate (pH 5.5), 1 μ M ECS and 10 μ M peptide substrate. Fluorescence levels were monitored using a Cytation3 cell imaging reader (BioTek) with excitation and emission filters of 328 and 393 nm, respectively. To investigate the effect of pH, ECS proteolytic activity was measured with different assay buffers: 50 mM sodium citrate–sodium phosphate (pH 3.0), 50 mM sodium acetate (pH 4.0–5.5), 50 mM sodium phosphate (pH 6.0–7.0) and 50 mM Tris-HCl (pH 7.5–8.5). To investigate the effect of temperature, ECS proteolytic activity was monitored in 50 mM sodium acetate buffer (pH 5.5) at reaction temperatures ranging from 25 °C to 60 °C.

GST pull-down assay

LURE1.2 and PDF1.2 lacking the signal peptide sequence were cloned into the pET28a vector. Similarly, ECS1 and ECS2 lacking signal peptide sequences were cloned into the pGEX4T-1 vector. Each plasmid was transformed into *E. coli* BL21 (DE3) for recombinant protein expression. LURE1.2 and PDF1.2 protein expression, purification and refolding were performed as previously described³⁸. GST pull-down assays were performed using the Pierce GST Protein Interaction Pull-Down Kit (Thermo Fisher Scientific) according to the manufacturer's instructions. Eluted samples were subjected to SDS–PAGE and then transferred to nitrocellulose membranes for immunoblotting with anti-GST (1:2,000 dilution; Abcam) and anti-His (1:2,000 dilution; Abcam).

Statistical analysis and reproducibility

The dot and box-and-whisker plots were prepared using GraphPad Prism v.8.4.2. Student's *t*-test (two-side) and Tukey–Kramer multiple

comparison test were used for statistical analysis. All experiments in this study were performed independently at least three times. At least three independent transgenic lines were investigated for each gene construct and at least three ovules were analysed per stage and plant. Statistical source data are available online, and Supplementary Fig. 1 displays the source data for gel images.

Reporting summary

Further information on research design is available in the Nature Research Reporting Summary linked to this paper.

Data availability

Published RNA sequencing data (Gene Expression Omnibus (GEO) accession numbers GSE121003, GSE33713, GSE32318, GSE102694 and GSE87760) were used for expression analysis in the present study. The raw data for the graphs that support the findings of this study are available online, and uncropped gel images are shown in the Supplementary Information file. The seeds of the transgenic lines described in this report are available from the corresponding authors on request. Source data are provided with this paper.

34. Wu, J. J. et al. Mitochondrial GCD1 dysfunction reveals reciprocal cell-to-cell signaling during the maturation of *Arabidopsis* female gametes. *Dev. Cell* **23**, 1043–1058 (2012).
35. Lampropoulos, A. et al. GreenGate—a novel, versatile, and efficient cloning system for plant transgenesis. *PLoS ONE* **8**, e83043 (2013).
36. Nelson, B. K., Cai, X. & Nebenführ, A. A multicolored set of in vivo organelle markers for co-localization studies in *Arabidopsis* and other plants. *Plant J.* **51**, 1126–1136 (2007).
37. Zhang, X., Henriques, R., Lin, S. S., Niu, Q. W. & Chua, N. H. Agrobacterium-mediated transformation of *Arabidopsis thaliana* using the floral dip method. *Nat. Protoc.* **1**, 641–646 (2006).
38. Wang, T. et al. A receptor heteromer mediates the male perception of female attractants in plants. *Nature* **531**, 241–244 (2016).
39. Sparkes, I. A., Runions, J., Kearns, A. & Hawes, C. Rapid, transient expression of fluorescent fusion proteins in tobacco plants and generation of stably transformed plants. *Nat. Protoc.* **1**, 2019–2025 (2006).
40. Soares, A. et al. An atypical aspartic protease modulates lateral root development in *Arabidopsis thaliana*. *J. Exp. Bot.* **70**, 2157–2171 (2019).
41. Zhao, P. et al. Two-step maternal-to-zygotic transition with two-phase parental genome contributions. *Dev. Cell* **49**, 882–893 (2019).

Acknowledgements We thank F. Berger for the HTR10–mRFP marker line, Y. Zhang for the *LAT52::DsRed* maker line, C. Li for the *LAT52::GUS* maker line and W. Li for help with the mammal cell expression system. This work was supported by the National Natural Science Foundation of China (31991201) and the German Research Council DFG via SFB960.

Author contributions M.-x.S., X.Y. and T.D. designed the research plan. X.Z., X.P., H.C. and C.S. performed the phenotype and genetics analyses. X.Y. and P.Z. performed the biochemical study. A. Bazhenova performed the in situ hybridization study. A. Bleckmann performed the cortical network observation study. T.D. and M.-x.S. contributed to the data analysis and finalized the manuscript. All authors contributed to the data collection, presentation and manuscript writing.

Competing interests The authors declare no competing interests.

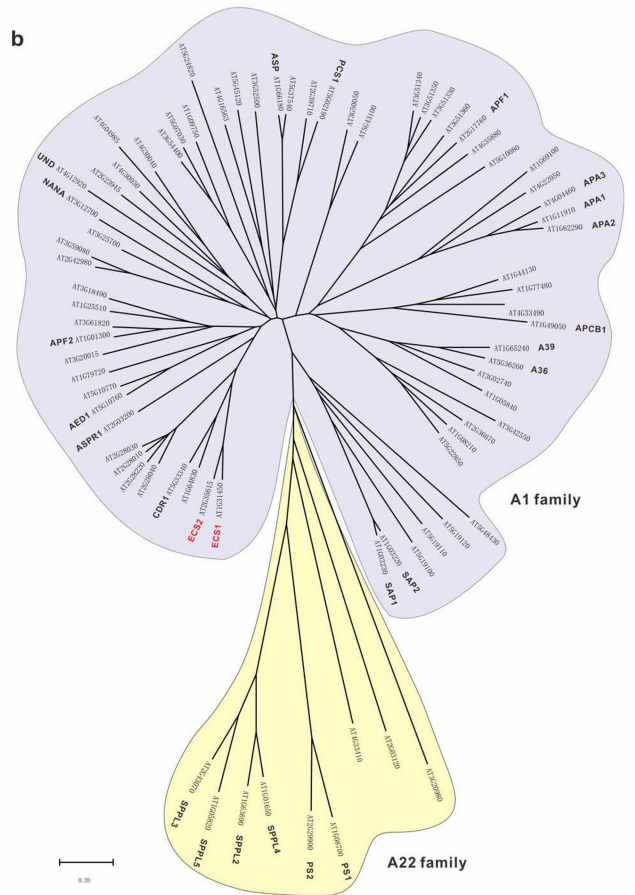
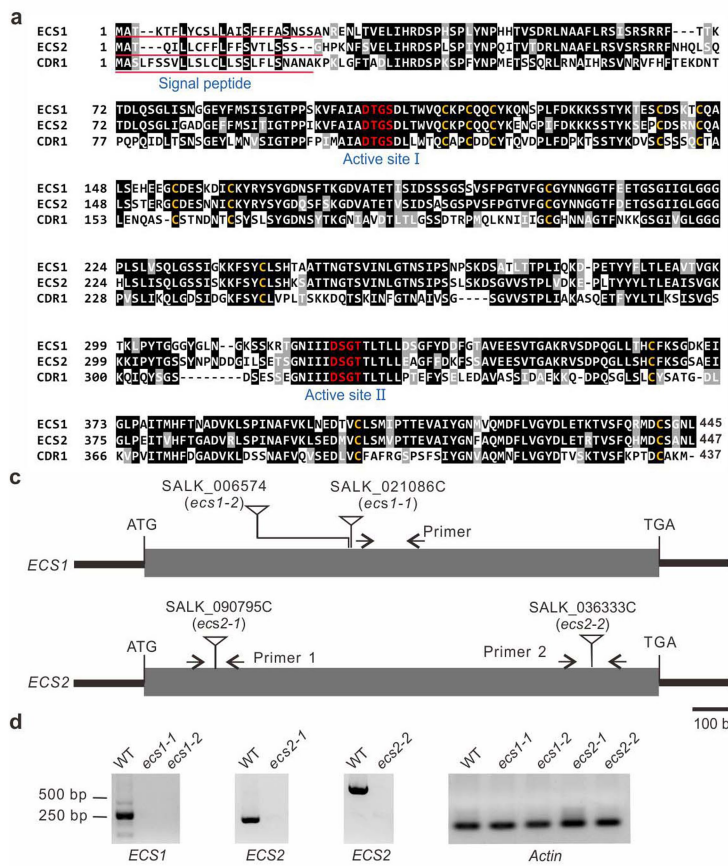
Additional information

Supplementary information The online version contains supplementary material available at <https://doi.org/10.1038/s41586-021-03387-5>.

Correspondence and **requests for materials** should be addressed to T.D. or M.-x.S.

Peer review information Nature thanks the anonymous reviewer(s) for their contribution to the peer review of this work.

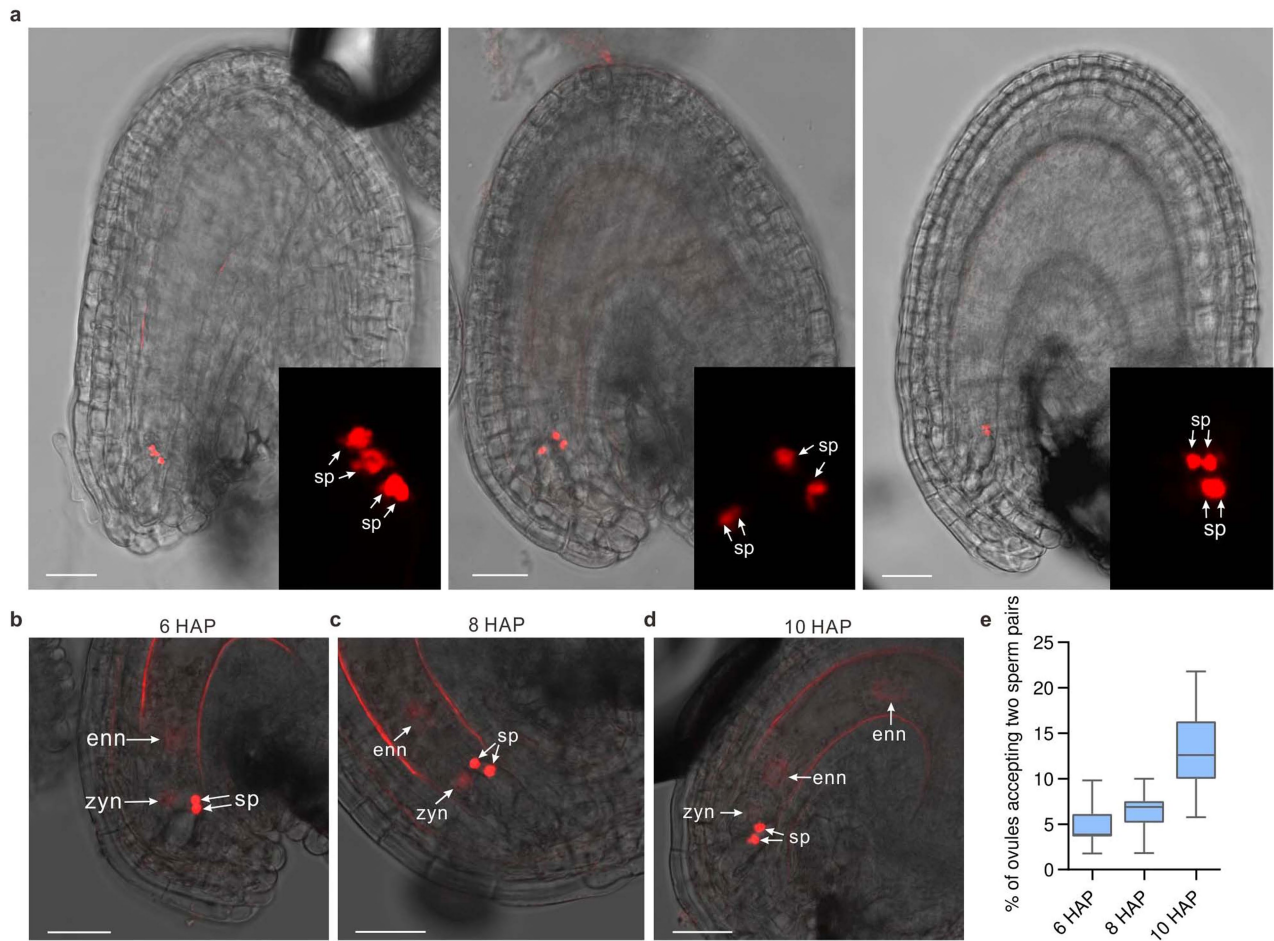
Reprints and permissions information is available at <http://www.nature.com/reprints>.



Extended Data Fig. 2 | Characteristics of ECS protein sequences, identification of their T-DNA insertion mutants and phylogenetic tree of aspartic endopeptidases in *Arabidopsis*. **a**, Alignment of ECS1/2 and CDR1 protein sequences. Two active sites and an N-terminal signal peptide are indicated. Conserved cysteines typical for aspartic proteases are labelled in yellow. **b**, Protein sequences of 78 aspartic proteases from *A. thaliana* annotated in the MEROPS database (<https://merops.sanger.ac.uk/>) were

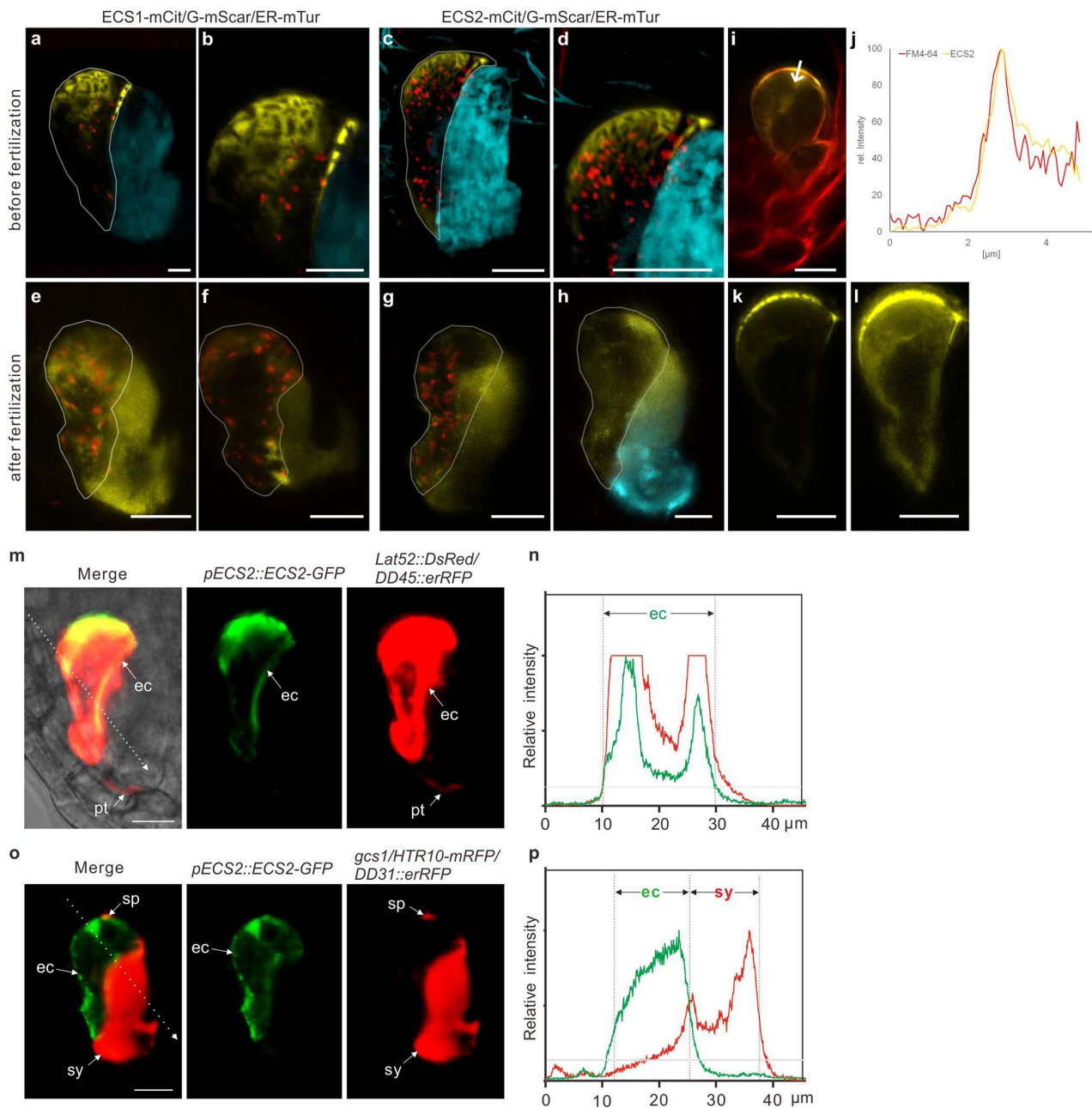
subjected to phylogenetic analysis by MEGA X. The phylogenetic tree was constructed using the Neighbour-Joining method. ECS1 and ECS2 are indicated in red. **c**, Scheme showing T-DNA insertion sites of *ecs1* and *ecs2* mutants.

d, RT-PCR using primers indicated in **b** revealed that transcripts levels of *ECS1* and *ECS2* were significantly reduced in their corresponding T-DNA insertion mutants. Actin was used as a control for RT-PCR analysis.



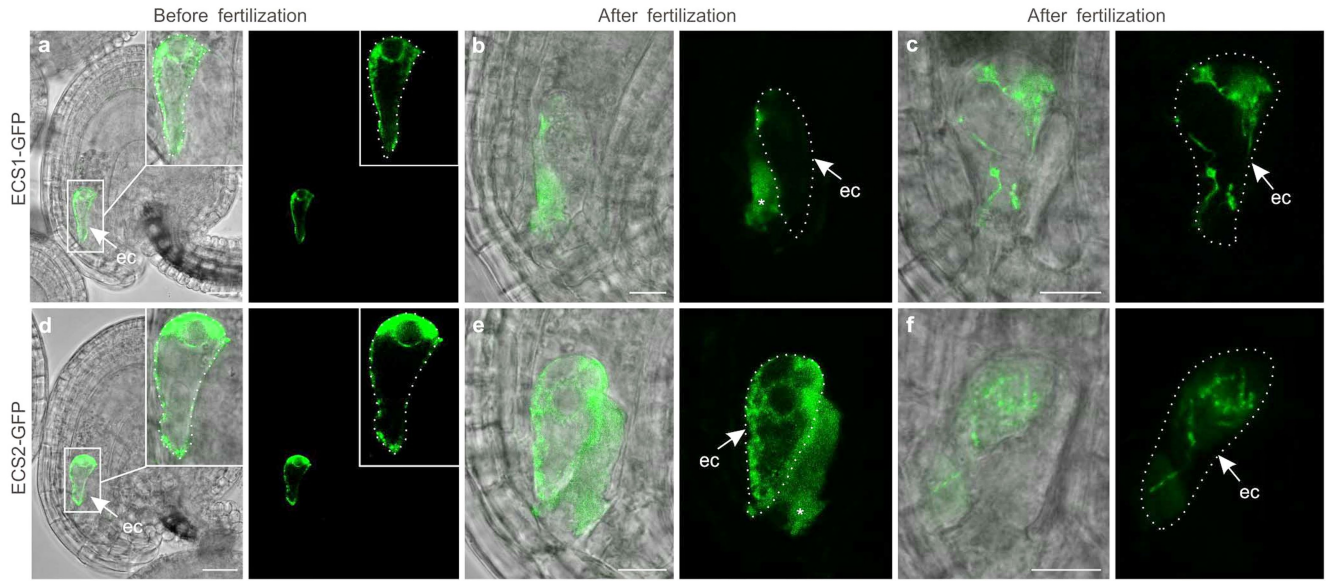
Extended Data Fig. 3 | As a consequence of polytubey, multiple sperm cell pairs are released in *ecs1 ecs2* mutant ovules. a, Three representative images showing two additional sperm cell pairs at 24 HAP, respectively. **b–d**, Time series showing representative images of two additional sperm cell pairs at 6 HAP (**b**), 8 HAP (**c**) and 10 HAP (**d**), respectively. **e**, Proportions of additional

sperm pairs in ovules of *ecs1 ecs2* mutants after fertilization ($n = 1056$ for 6 HAP; 1114 for 8 HAP, 1083 for 10 HAP). Data are presented in box-and-whisker plots. Bottom and top of the box, 25th and 75th percentiles; centre line, 50th percentile; whiskers, minimum and maximum data. Abbreviations: sp., sperm cell; enn, endosperm nucleus; zyn, zygote nucleus. Scale bars, 20 μ m.



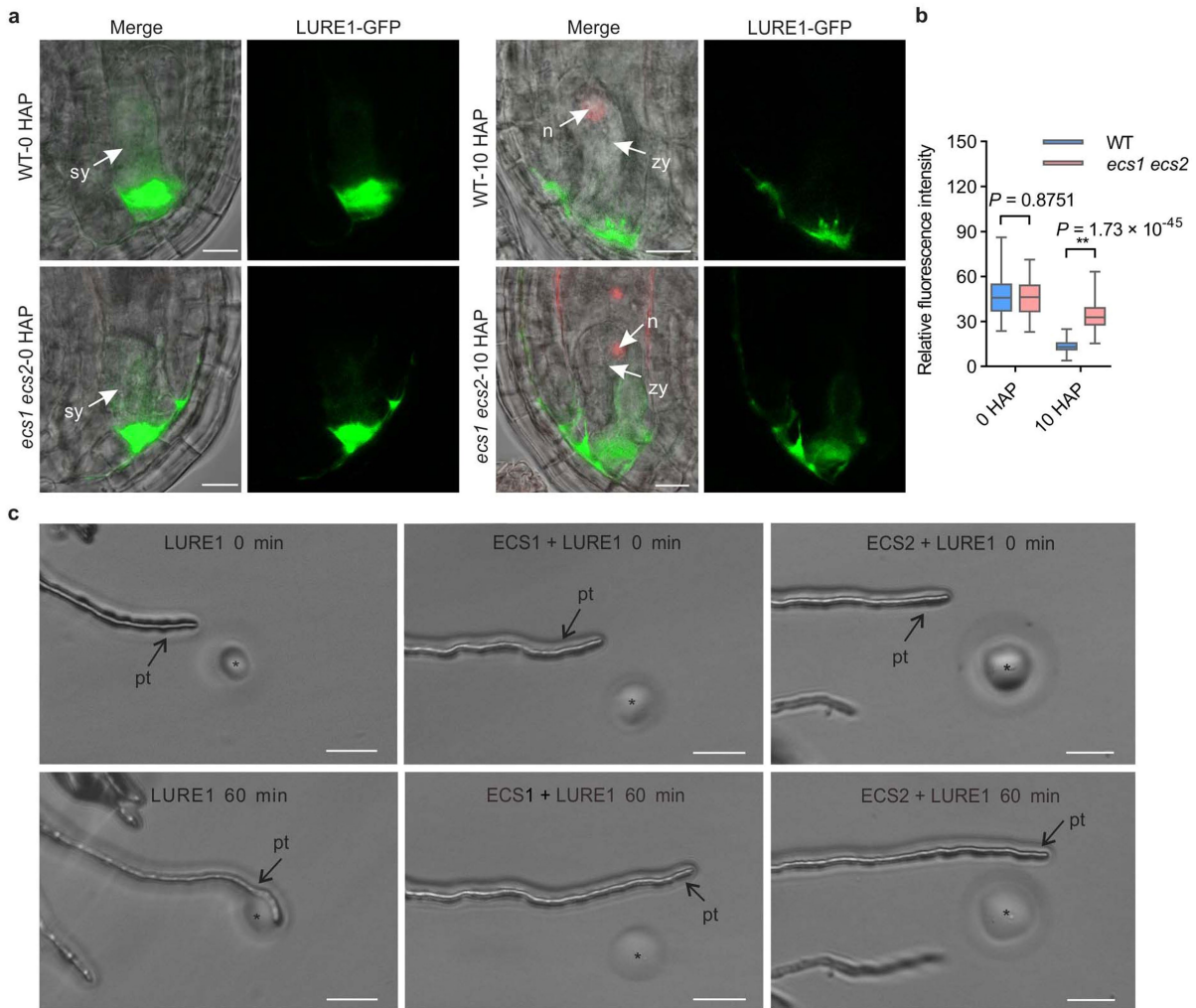
Extended Data Fig. 4 | ECS1 and ECS2 are almost quantitatively secreted from an apical network of the mature egg cell to the extracellular space only after gamete fusion. a, b, ECS1-mCitrine (mCit) at the apical domain forming a network before fertilization. **c, d**, ECS2-mCit accumulate at the apical domain forming a network before fertilization. **b, d**, Enlargement of apical domains of egg cells shown in **a, b**. **e–h**, ECS1-mCit (**e, f**) and ECS2-mCit (**g, h**) are secreted from the egg cell to the extracellular space. Synergids are largely degenerated as indicated by the lack or diminished signal of the synergid marker. Volume projections of z-stacks from ECS1/2-mCit (yellow), an egg cell expressed Golgi-mScarlet (mScar; red) and a synergid expressed endoplasmic reticulum marker tagged to mTurquoise2 (mTur; cyan) are shown. **i**, FM4-64 staining showing that the cortical network containing ECS2-mCit is located at the plasma membrane. **j**, Signal intensity plot along the arrow shown in **i** indicates that ECS2-Cit is located at or just below the plasma membrane. **k**, Single optical section through the cortical network shows weak ECS2-Cit

signals outside the network. **l**, Overexposure of the same optical section shown in **k** illustrates ECS2-Cit signals throughout the egg cytoplasm. **m**, Overexposed image showing ECS2-GFP accumulating in the apical egg cell domain and the endoplasmic reticulum marker EC1.2::erRFP marking the boundaries of the egg cell. A pollen tube expressing DsRed driven by the *Lat52* promoter was used to monitor pollen tube perception. During pollen tube arrival ECS2-GFP was not yet released. **n**, Intensity plot profile showing relative fluorescence signal intensities of ECS2-GFP (green line) and erRFP (red line) along a dashed line drawn across the egg cells (indicated in the left image) confirming the microscopic observation. **o**, Sperm cells defective in gamete fusion (*gcs1* mutant) did not trigger ECS2-GFP release. **p**, Intensity plot profile as in **n** showing that egg cell-localized ECS2-GFP and synergid cell-localized erRFP signals do not overlap. Ec, egg cell; pt, pollen tube; sp., sperm cells; sy, synergid cells. Scale bars, 10 μm.



Extended Data Fig. 5 | Truncated ECS1 and ECS2 proteins are not secreted from egg cells during fertilization. **a, d**, ECS1-GFP and ECS2-GFP were located inside the egg cell before fertilization. **b, e**, ECS1-GFP and ECS2-GFP were secreted from the egg cell at 8 HAP. Asterisks mark secreted ECS1-GFP

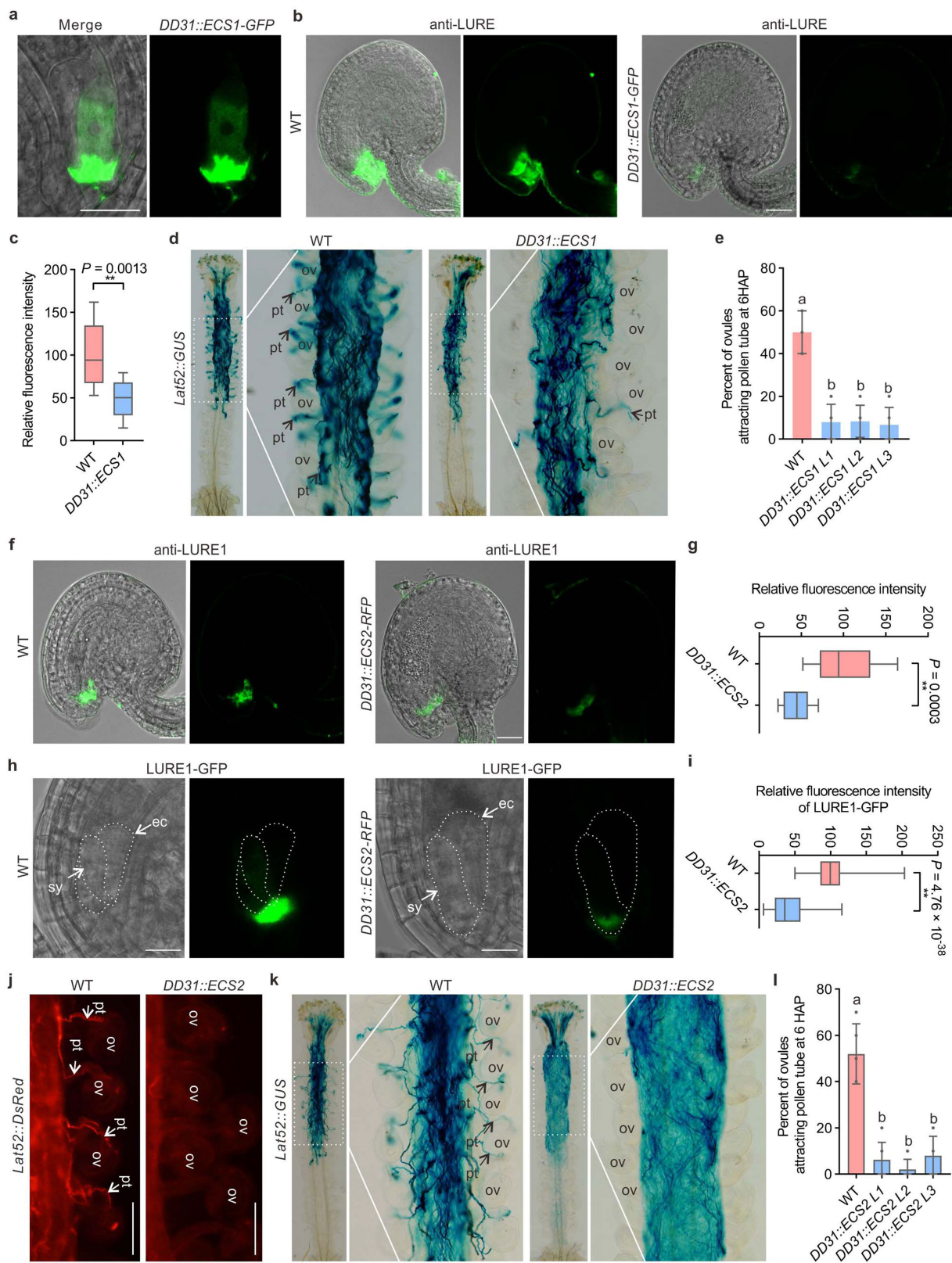
and ECS2-GFP, respectively. **c, f**, Truncated TECS1-GFP (**c**) and TECS2-GFP (**f**) versions lacking signal peptides could not be secreted from the egg cell at 8 HAP. *ec*, egg cell. Dashed lines outline the egg cell boundaries. Insets show enlargements of regions indicated. Scale bars, 20 μ m.



Extended Data Fig. 7 | ECS1 and ECS2 efficiently cleave LURE1 substrates.

a, Localization and protein level of LURE1.2-GFP before pollination and in fertilized ovules of WT and *ecs1 ecs2* mutant pistils, respectively. Pistils were pollinated with pollen expressing HTR10-mRFP in sperm cells. Ovules were collected from pistils at 0 and 10 HAP. *ecs1 ecs2* mutation resulted in the accumulation of LURE1.2 after fertilization. **b**, Quantification of green fluorescence intensity in ovules from WT and *ecs1 ecs2* pistils ($n = 101$). Data for fluorescence intensity are presented in box-and-whisker plots. Bottom and top of the box, 25th and 75th percentiles; centre line, 50th percentile; whiskers,

minimum and maximum data. ** indicates statistically significant difference between WT and mutant ovules (two-tailed Student's *t*-test; $P < 0.01$). **c**, In vitro pollen tube attraction assay with gelatin beads containing ECS1- and ECS2-digested LURE1.2, respectively. Beads (*) were prepared using 1 μ M LURE1.2 alone and in combination with 1 μ M ECS1 and ECS2, respectively, and placed close to growing pollen tube tips (0 min) and observed for 60 min. Pollen tube attraction activity was lost when beads contained both, LURE1.2 and ECS endopeptidases. n, nucleus; pt, pollen tube; sy, synergid cell; zy, zygote. Scale bars are 10 μ m (**a**) and 50 μ m (**c**).



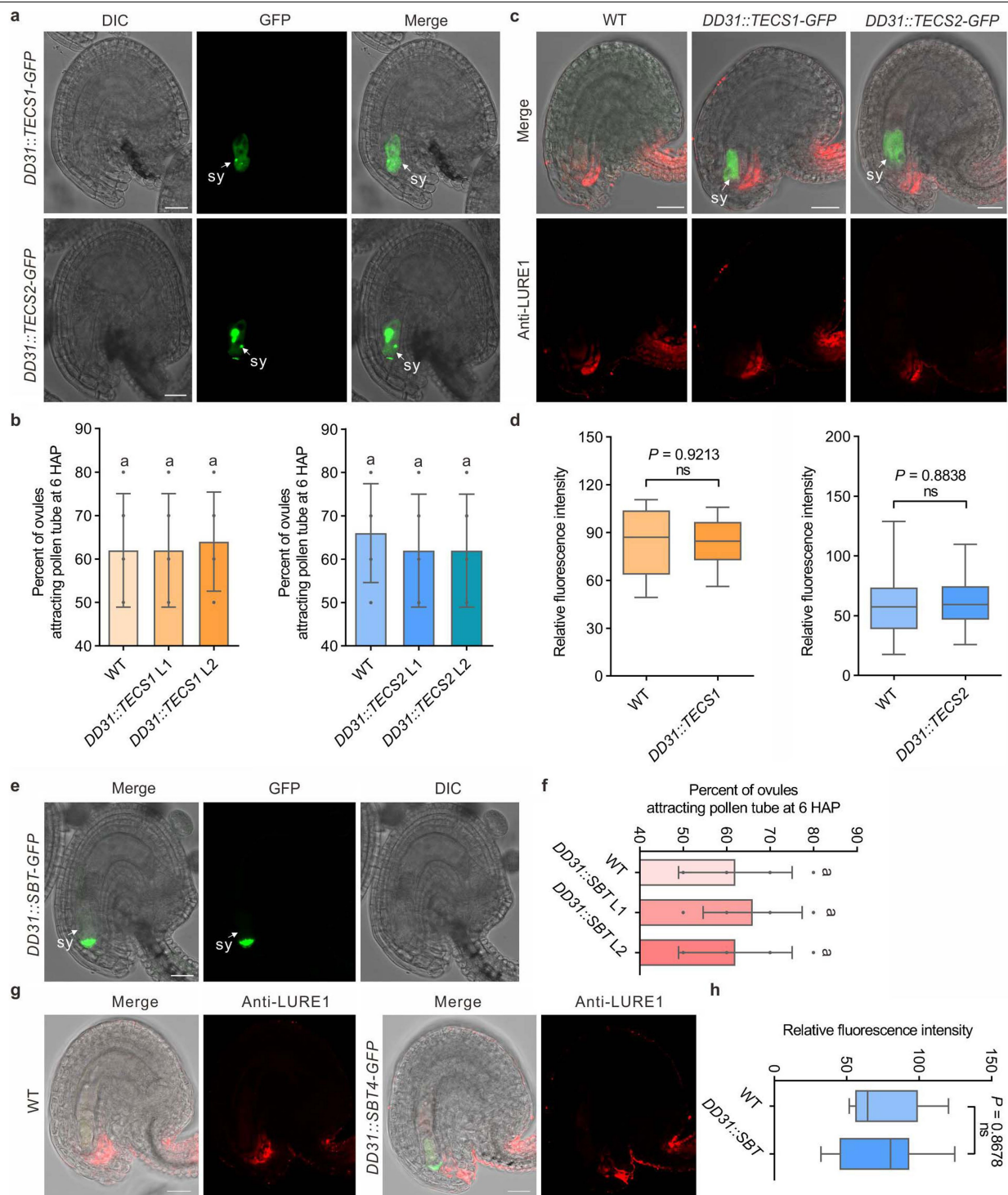
Extended Data Fig. 8 | See next page for caption.

Article

Extended Data Fig. 8 | Ectopic expression of *ECS1* and *ECS2* in synergid cells leads to a decrease of LURE1.2 protein levels and strongly reduced pollen tube attraction rate.

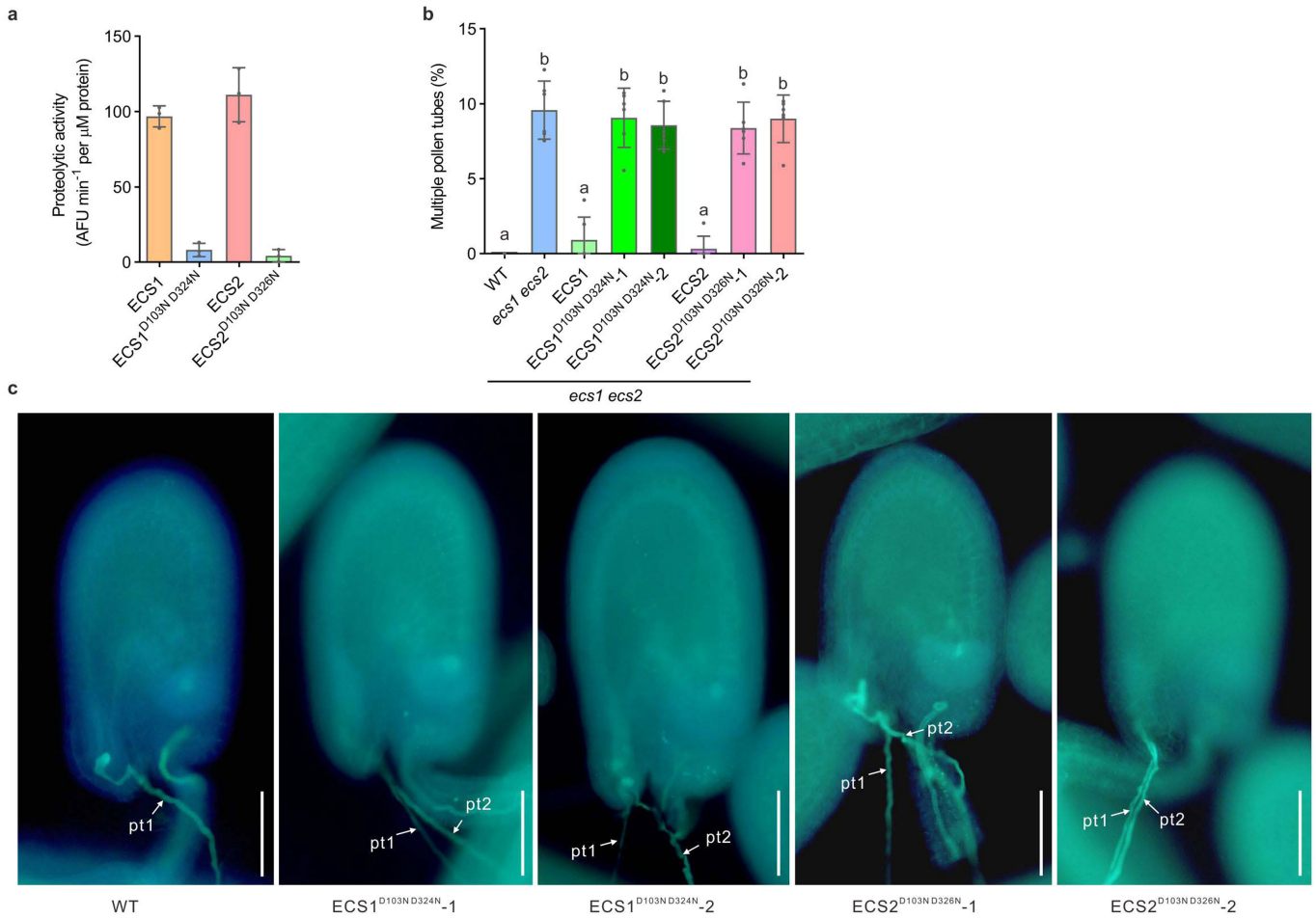
a, Ectopically expressed *ECS1*-GFP fusion protein in synergid cells is secreted to the filiform apparatus. **b**, Immunofluorescence revealed that LURE1 levels were significantly decreased in ovules ectopically expressing *ECS1-GFP* in synergid cells using the *DD31* promoter. **c**, Quantification of LURE1 fluorescence intensity in WT and *ECS1*-ectopically expressed ovules as shown in (b) ($n = 10$). **d**, Ectopic expression of *ECS1* in synergid cells resulted in pollen tube attraction defects 6 HAP. Pollen tube growth analysis was performed using a *Lat52::GUS* reporter line. **e**, Percentages of ovules attracting pollen tubes observed in WT pistils and those ectopically expressing *ECS1* in synergid cells of three independent lines (L1–L3) at 6 HAP ($n = 50$ for WT and *DD31::ECS1L1*; 60 for *DD31::ECS1L2* and *DD31::ECS1L3*). **f**, Immunofluorescence revealed that LURE1 levels were significantly decreased in ovules ectopically expressing *ECS2* in synergid cells using the *DD31* promoter. **g**, Quantification of LURE1 fluorescence intensity in WT ovules and those

ectopically expressing *ECS2* ($n = 10$). **h**, Similarly, LURE1.2-GFP signals were significantly decreased in ovules ectopically expressing *ECS2* in synergid cells. **i**, Quantification of LURE1.2-GFP fluorescence intensity as described in **b** ($n = 101$). **j**, **k**, Ectopic expression of *ECS2* in synergid cells resulted in reduction of pollen tube attraction 6 HAP. *Lat52::DsRed* (**j**) and *Lat52::GUS* reporter line (**k**) were used in this analysis. **l**, Proportions of ovules attracting pollen tubes observed in WT plants and those ectopically expressing *ECS2* in synergid cells at 6 HAP ($n = 50$ for WT, *DD31::ECS2L2* and *DD31::ECS2L3*; 80 for *DD31::ECS2L1*). Data in **c**, **g**, **i** are presented in box-and-whisker plots. Bottom and top of the box, 25th and 75th percentiles; centre line, 50th percentile; whiskers, minimum and maximum data. ** indicates statistical difference compared to WT (Two-tailed Student's *t*-test; $P < 0.01$). Same letters (in **e** and **l**) indicate lack of significant differences according to the Tukey–Kramer multiple comparison test (one-way ANOVA between groups; $P = 1.94 \times 10^{-7}$; $F = 32.11$ in **e**; $P = 3.24 \times 10^{-8}$, $F = 37.88$ in **l**). $P < 0.05$ was considered as significant. Scale bars, 20 μm (**a**, **b**, **f**, **h**), 100 μm (**j**). ec, egg cell; sy, synergid; pt, pollen tube; ov, ovule.



Extended Data Fig. 9 | Ectopic expression of truncated versions of *ECSI* and *ECS2* or the subtilisin-like protease *SBT4.13* in synergid cells have no significant influence on *LURE1.2* protein levels and pollen tube attraction rate. **a, Ectopic expressions of truncated versions of *ECSI* and *ECS2* (*TECS1/2*) in synergid cells. **b**, Proportions of ovules attracting pollen tubes observed in WT plants and those ectopically expressing *TECS1/2* in synergid cells at 6 HAP ($n = 50$). **c**, Immunofluorescence revealed that *LURE1* levels were comparable in WT and ovules ectopically expressing *TECS1/2* in synergid cells using the DD31 promoter. **d**, Quantification of *LURE1* fluorescence intensity in WT ovules and those ectopically expressing truncated *TECS1/2* in synergid cells ($n = 10$). **e**, Ectopic expressions of the egg cell expressed subtilisin-like protease *SBT4.13*²⁷ as a GFP fusion protein in synergid cells. *SBT4.13*-GFP is secreted to the filiform apparatus. **f**, Proportions of ovules attracting pollen tubes**

observed in WT plants and those ectopically expressing *SBT4.13* in synergid cells at 6 HAP ($n = 50$). **g**, Immunofluorescence revealed that *LURE1* levels were comparable in WT and ovules ectopically expressing *SBT4.13* in synergid cells. **h**, Quantification of *LURE1* fluorescence intensity in WT ovules and those ectopically expressing *SBT4.13* ($n = 10$). Data in **b**, **f** represent the mean \pm s.d. Same letters in **b**, **f** indicate lack of significant differences according to the Tukey-Kramer multiple comparison test (one-way ANOVA between groups; $P = 0.96$, $F = 0.04$ in **b** left plane; $P = 0.85$, $F = 0.17$ in **b** right plane; $P = 0.85$, $F = 0.17$ in **f**). $P < 0.05$ was considered as significant. Data in **d**, **h** are presented in box-and-whisker plots. Bottom and top of the box, 25th and 75th percentiles; centre line, 50th percentile; whiskers, minimum and maximum data. Two-tailed Student's *t*-test was used for statistical test in **d**, **h**. ns, no significant differences. sy, synergid cell. Scale bars, 20 μ m.



Extended Data Fig. 10 | Mutation of active sites of ECS1 and ECS2 endopeptidases leads to polytubey. **a**, Mutation of active sites of ECS1 and ECS2 (Extended Data Fig. 2a) led to reduced proteolytic activity. Proteolytic activities of recombinant WT and mutant version of ECS towards cleavage of fluorogenic peptide 3 (Extended Data Fig. 6) were measured respectively. Data represent mean \pm s.d. of three independent experiments. **b**, Mutant version of ECS could not recover the polytubey phenotype of *ecs1 ecs2* double mutant. Proportions of polytubey in *ecs1 ecs2* double mutants and different transgenic

lines were determined at 24 HAP ($n = 308$ for WT; 302 for *ecs1 ecs2*; 309 for ECS1; 319 for ECS1^{D103N D324N}-1; 302 for ECS1^{D103N D324N}-2; 309 for ECS2; 321 for ECS2^{D103N D326N}-1; 300 for ECS2^{D103N D326N}-2). Data represent the mean \pm s.d. Same letters indicate lack of significant differences according to the Tukey-Kramer multiple comparison test (one-way ANOVA between groups; $P = 7.82 \times 10^{-18}$, $F = 50.24$). $P < 0.05$ was considered as significant. **c**, Representative images showing multiple pollen tubes entrance in different transgenic lines as indicated. Arrows indicate pollen tubes (pt). Scale bars, 100 μ m.